

## Photocurrent spectroscopy of site-controlled pyramidal quantum dots

A. Mohan,<sup>1,a)</sup> L. Nevou,<sup>1</sup> P. Gallo,<sup>2</sup> B. Dwir,<sup>2</sup> A. Rudra,<sup>2</sup> E. Kapon,<sup>2</sup> and J. Faist<sup>1,b)</sup>

<sup>1</sup>*Institute for Quantum Electronics, Wolfgang-Pauli-Strasse 16, ETH Zürich, 8093 Zürich, Switzerland*

<sup>2</sup>*Laboratory of Physics of Nanostructures, Ecole Polytechnique Fédérale de Lausanne, 1015 Lausanne, Switzerland*

(Received 19 April 2012; accepted 2 July 2012; published online 18 July 2012)

Intraband photocurrent spectroscopy of site-controlled pyramidal quantum dots by inserting them into the intrinsic region of n-i-n like quantum dot infrared photodetector structure is reported. The photovoltaic response is observed in the mid-infrared region. A peak responsivity of 0.4 mA/W at 120 meV ( $\lambda = 10 \mu\text{m}$ ) is observed at 10 K at  $-2$  V bias. The ability to engineer states in the conduction band of the QDs has been exploited to tune their photocurrent response from  $10 \mu\text{m}$  to  $18 \mu\text{m}$  with a narrow spectral width of  $\Delta\lambda/\lambda = 0.17$ . © 2012 American Institute of Physics. [<http://dx.doi.org/10.1063/1.4737426>]

Infrared photodetectors based on quantum dots (QDs), commonly called as quantum dot infrared photodetectors (QDIPs), have been studied extensively.<sup>1–7</sup> The discrete nature of the density of states provided by the QDs are responsible for many of the attractive properties like sensitivity to normal-incidence radiation, low dark current levels, potentially high operating temperatures<sup>8,9</sup> with respect to its counterparts, the quantum well based infrared photodetectors (QWIPs). Currently studied QDIPs are solely based on the self-assembled QDs commonly called, Stranski-Krastanow (S-K) QDs.<sup>10</sup> The strain driven formation of these QDs limits the control over the QD shape, size, and composition profile. This inherent randomness results in a lack of control over the spectral response obtainable from these QDIPs. In contrast, the QDs grown into site-controlled pyramidal QDs have low inhomogeneous broadening<sup>11</sup> and finely tunable emission energy.<sup>12</sup> Although the lower density of the pyramidal QDs limits the performance as a QDIP, the site-control enables the use of pyramidal QD based photodetectors in applications like the electron pump.<sup>13</sup>

Here, we report on the intraband photocurrent spectroscopy of site-controlled pyramidal QDs. The investigated semiconductor QDs reported here were grown by low-pressure (20 mbar) metal-organic chemical vapor deposition (MOCVD). A planar layer of 50 nm of n-doped ( $5 \times 10^{18} \text{cm}^{-3}$ ) GaAs:Si was regrown on a semi-insulating (111)B GaAs substrate to form the bottom contact, followed by a 500 nm undoped GaAs. This layer was then patterned with 500 nm pitch hexagonal arrays of inverted, tetrahedral pyramids of size 230 nm using electron beam lithography and wet chemical etching which leads to a QD density of  $5 \times 10^8 \text{cm}^{-2}$ .<sup>11</sup> The grown structures inside the pyramids consisted of a 1.3 nm thick GaAs buffer layer, 5 nm GaAs layer (inferior cladding), an  $\text{In}_{0.15}\text{Ga}_{0.85}\text{As}$  QD layer of 0.6 nm thickness, a 1 nm GaAs layer (superior cladding), a 0.5 nm  $\text{Al}_{0.3}\text{Ga}_{0.7}\text{As}$  current blocking layer followed by a 15 nm n-doped ( $2 \times 10^{18} \text{cm}^{-3}$ ) GaAs:Si, all layers were grown at 590 °C. All thicknesses refer to growth on planar (100) substrates; the actual QD thickness is  $\sim 9$  times thicker (as determined by cross-sectional AFM images) due to

capillarity effects in the pyramids formed into the 111 B substrate.<sup>14</sup> As a result of this growth, QDs are formed at the apex of the pyramid and lateral quantum wires (LQWRs) are formed at the three vertices of the pyramid as described in Ref. 11.

The conduction band profile (simulated with 1D self-consistent Poisson-Schrödinger Solver) of the sample is shown in Fig. 1(a). In this design, the n-doped GaAs (top-contact) is used as a reservoir of electrons to feed the QDs. The AlGaAs barrier between the top-contact and the QD serves to block the dark current. The electrons that populate the QDs are optically excited into the LQWR and into the continuum. The active region reported here is similar to the strongly asymmetric structure reported in Ref. 15. A long spacer between the QD layer and the back contact provides a potential slope for the electrons to reach the back contact even at 0 V bias and hence the photocurrent can be generated in the photovoltaic mode.

The interband optical emission properties of these QDs were studied using conventional micro-PL ( $\mu\text{PL}$ ) setups. The sample was mounted in a He-flow cryostat and kept at a constant temperature near 10 K. The QDs were optically excited by a frequency-doubled diode-pumped Nd:YVO4 laser at  $\lambda = 532 \text{nm}$  in continuous wave for non-resonant PL. The spatial resolution was  $\sim 1 \mu\text{m}$  and the spectral resolution was set at  $90 \mu\text{eV}$ . The inset of Fig. 2 shows PL measurements performed on the sample at low temperature (10 K) for different excitation powers. At low optical excitation, emission is detected mainly from the ground state (1.313 eV) of the QDs. By increasing excitation power; emission from carriers in higher confined levels is observed. This effect is consistent with the state-filling picture often used for QDs.<sup>16</sup> The peak at 1.445 eV is attributed to the LQWR, which acts as the barrier to the QD.

To determine the photocurrent, these QDs were incorporated into an n-i-n structure as shown in Fig. 1(b). The sample was processed into mesas of  $780 \mu\text{m}^2$  by wet chemical etching. As an Ohmic back contact, Ni/Ge/Au/Ni/Au (10 nm/40 nm/80 nm/200 nm) was deposited and subsequently annealed at 400 °C for 1 min. To increase the probability of injection into the QDs, the top contact was selectively formed only above the QDs by electron beam lithography using  $\text{SiO}_2$  as a hard mask. To avoid Ge diffusion

<sup>a)</sup>amohan@phys.ethz.ch.

<sup>b)</sup>faist@ethz.ch.

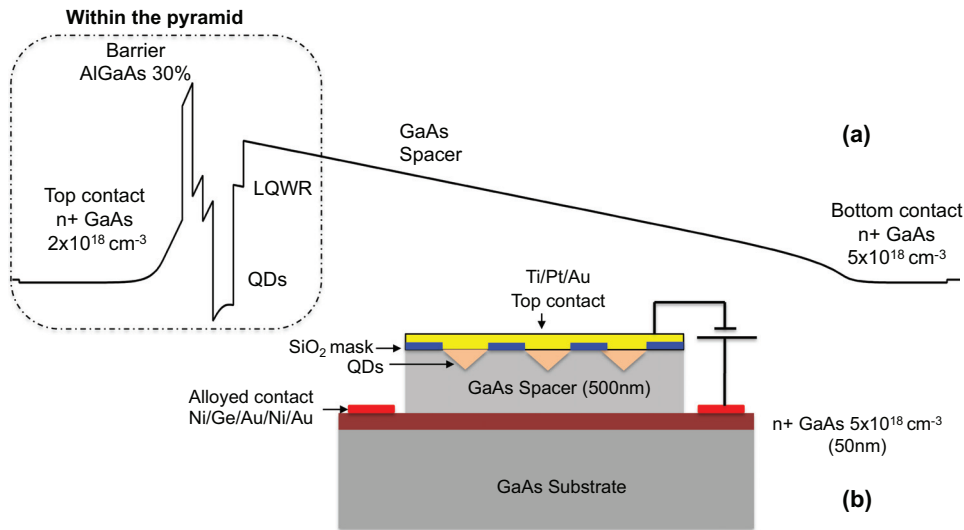


FIG. 1. Sketch of the conduction band profile of the photodetector. (Inset) Sketch of the pyramidal QD embedded in an n-i-n like QDIP structure.

into the QD, a top contact of Ti/Pt/Au (5 nm/50 nm/200 nm) was evaporated. To subsequently perform photocurrent spectroscopy, the facet of the sample was mechanically polished at  $45^\circ$  at the entrance, so that a component of the electric field can be couple along the growth axis (p-polarized light). A vacuum Fourier transform infrared (FTIR) spectrometer was used in rapid-scan mode with a low noise current amplifier (Stanford SR570). The FTIR was equipped with a black-body glow-bar, KBr beam splitter and KBr windows and the sample was mounted in a flow-cryostat and measured at a temperature of 10 K.

The resulting photocurrent spectrum illustrated in Figure 2 depicts two distinct peaks. The peak at 120 meV ( $10 \mu\text{m}$ ) is attributed to the absorption of an electron from the ground state of the QD to the LQWR. From the PL (Figure 2 inset), it is seen that the energy separation between the ground state of the QD to the LQWR is 132 meV; the  $\sim 12$  meV difference between the two corresponds to a possible separation of the hole states of the QD and LQWR. Again from PL, the energy separation of the ground state of the QD to the GaAs peak at 1.52 eV corresponds to 207 meV. Taking into account the valence band offsets of the QD with GaAs ( $\sim 80$  meV), the broader peak in the pho-

tocurrent spectra of Figure 2 at 160 meV ( $7.6 \mu\text{m}$ ) is attributed to the absorption of the ground state of the QD to the continuum. The peaks in the photocurrent spectra are thus in conjunction to the peaks observed in PL. The ratio of the photocurrent recorded for polarizations perpendicular (p) and parallel (s) to the growth direction is around  $\sim 3.5$  in agreement with values already observed for QDIPs.<sup>17</sup> Although it is to be noted that this is not the true absorption strength for the two polarizations as the metal at the surface also influences the polarization selection.

In order to calibrate the responsivity, we illuminated the sample with a quantum cascade laser (QCL) with an average power of 1 mW emitting at  $\lambda = 10 \mu\text{m}$ , that corresponds to the absorption of electrons from the QD to the LQWR (refer Fig. 2). The responsivity spectrum (refer Fig. 3) peaks at 0.4 mA/W at  $-2$  V ( $10 \mu\text{m}$ ) and is  $0.85 \mu\text{A/W}$  with no bias (photovoltaic regime). The peak responsivity of the best single layer photovoltaic QDIP based on self-assembled QDs is 6 mA/W.<sup>15</sup> The responsivity of QDIPs is directly proportional to the number of QDs,<sup>8</sup> the density of the pyramidal QDs is at least two orders of magnitude ( $\sim 5 \times 10^8 \text{ cm}^{-2}$ ) lower than the self-assembled QDs. The fact that the responsivity of the device reported here is only a factor 15 lower than in Ref. 15, which implies that the quantum efficiency normalized to the number of QDs is  $\sim 3$  more for the devices presented here. This is explained by the higher ( $\times 3$  compared to Ref. 15) effective absorption cross-section ( $\sigma$ ) of the QDIP presented here due to the low inhomogeneous broadening of the pyramidal QDs. From the peak responsivity, the  $\sigma$  of the QDIPs is estimated to be  $5.2 \times 10^{-14} \text{ cm}^{-2}$  at  $-2$  V and at 0 V bias when the extraction efficiency is low the  $\sigma$  is estimated to be  $1.5 \times 10^{-16} \text{ cm}^{-2}$ .

The pyramidal QD system enables excellent control over the QD shape and size,<sup>18</sup> such control facilitates engineering the energy level spacing<sup>19</sup> within the conduction band of the QD. To exploit this ability, QDs with varying energy separation of the ground state of the QD to the LQWR were fabricated. Figure 3(b) shows the PC response of the QDIPs formed by such pyramidal QDs. The response is tunable almost continuously from  $10 \mu\text{m}$  to  $18 \mu\text{m}$ . The biggest advantage of this system is that the tuning reported here is achieved in a single growth run, i.e., the composition

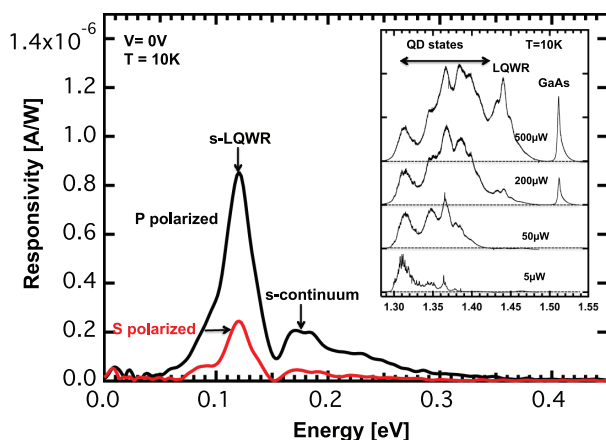


FIG. 2. Photovoltaic photocurrent spectra for p and s polarization of the QDIP. (Inset) Photoluminescence spectra of the QD sample under varied excitation powers. The dashed lines in the inset correspond to the zero line of each spectrum.

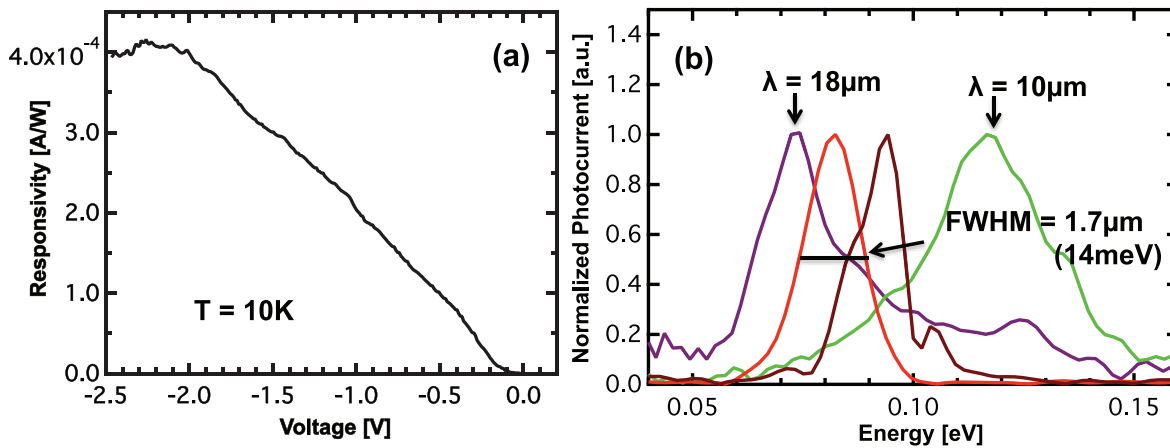


FIG. 3. (a) Photocurrent responsivity at 10K of 0.4 mA/W at bias of  $-2$  V calibrated with a QCL at  $10\ \mu\text{m}$ . (b) Tuning of the photocurrent response from  $10\ \mu\text{m}$  to  $18\ \mu\text{m}$  by engineering states in the conduction band of the QD. Also shown is the low spread ( $\Delta\lambda/\lambda = 0.17$ ) in the photocurrent spectra.

of the QDs is kept constant but changing the pyramid size changes the size and shape of the QDs.<sup>19</sup> This feature enables multi-color IR detector arrays for high performance sensor applications.<sup>20</sup>

The broadening of the photocurrent spectra in a QDIP depends not just on the inhomogeneous broadening of the ground state of the QD but also of the state to which the electrons are absorbed. Nevertheless, it is reasonable to expect a low inhomogeneous broadening characteristic of the pyramidal QDs (Ref. 11) to result in a low broadening of the photocurrent spectra as well. This expectation was verified in the low photocurrent spread of 14 meV ( $1.7\ \mu\text{m}$ ) depicted in Figure 3(b), as opposed to a typically observed spreading of 30 meV in S-K QD based QDIPs.<sup>15</sup>

In conclusion, we have demonstrated QDIP based on site-controlled QDs. The tuning of the photocurrent response has been demonstrated from  $10\ \mu\text{m}$  to  $18\ \mu\text{m}$ , thanks to the ability to engineer states in the CB of these QDs. The superior spatial and spectral control of these pyramidal QDs must make them ideal candidates for integration with high finesse photonic cavities to improve response of these QDIPs.<sup>21</sup> Furthermore, Nevou *et al.*<sup>13</sup> proposed and demonstrated an electron-pump based on QDs optically pumped by a pulsed laser. In the proposed electron-pump, each dot is the equivalent to an SET device and millions of them can operate in parallel to produce a substantial current. The accuracy of such an electron-pump relies on extracting a known number of electrons from only the ground state of the QD. Site-controlled QDs with its low inhomogeneous broadening and a known number of QDs are thus an ideal candidate for increasing the accuracy of these e-pumps.

<sup>1</sup>S. Krishna, S. D. Gunapala, S. V. Bandara, C. Hill, and D. Z. Ting, *Proc. IEEE* **95**, 1838–1852 (2007).

<sup>2</sup>J. Jiang, S. Tsao, T. O'Sullivan, W. Zhang, H. Lim, T. Sills, K. Mi, M. Razeghi, G. J. Brown, and M. Z. Tidrow, *Appl. Phys. Lett.* **84**, 2166 (2004).

<sup>3</sup>S. Krishna, D. Forman, S. Annamalai, P. Dowd, P. Varangis, T. Tumolillo, Jr., A. Gray, J. Zilko, K. Sun, M. Liu, and J. Campbell, *Appl. Phys. Lett.* **86**, 193501 (2005).

<sup>4</sup>A. Rogalski, *J Mod Opt.* **57**(18), 1716–1730 (2010).

<sup>5</sup>D. Pan, E. Towe, and S. Kennerly, *Appl. Phys. Lett.* **76**, 3301 (2000).

<sup>6</sup>W. Q. Ma, X. J. Yang, M. Chong, T. Yang, L. H. Chen, J. Shao, X. Lü, W. Lu, C. Y. Song, and H. C. Liu, *Appl. Phys. Lett.* **93**, 013502 (2008).

<sup>7</sup>S. H. Hwang, J. C. Shin, J. D. Song, W. J. Choi, J. I. Lee, H. Han, and S.-W. Lee, *Microelectron. Eng.* **229**, 78–79 (2005).

<sup>8</sup>H.C. Liu, *Opto-Electron. Rev.* **11**, 1–5 (2003).

<sup>9</sup>V. Ryzhii, *Semicond. Sci. Technol.* **11**, 759 (1996).

<sup>10</sup>L. Goldstein, F. Glas, J. Y. Marzin, M. N. Charasse, and G. Leroux, *Appl. Phys. Lett.* **47**, 1099 (1985).

<sup>11</sup>A. Mohan, P. Gallo, M. Felici, B. Dwir, A. Rudra, J. Faist, and E. Kapon, *Small* **6**, 1268 (2010).

<sup>12</sup>M. Felici, P. Gallo, A. Mohan, B. Dwir, A. Rudra, and E. Kapon, *Small* **5**, 938 (2009).

<sup>13</sup>L. Nevou, V. Liverini, P. Friedli, F. Castellano, A. Bismuto, H. Sigg, F. Gramm, E. Müller, and J. Faist, *Nat. Phys.* **7**, 423 (2011).

<sup>14</sup>G. Biasiol and E. Kapon, *Phys. Rev. Lett.* **81**, 2962 (1998).

<sup>15</sup>L. Nevou, V. Liverini, F. Castellano, A. Bismuto, and J. Faist, *Appl. Phys. Lett.* **97**, 023505 (2010).

<sup>16</sup>P. Hawrylak, G. A. Narvaez, M. Bayer, and A. Forchel, *Phys. Rev. Lett.* **85**, 389 (2000).

<sup>17</sup>S. Sauvage, P. Boucaud, T. Brunhes1, V. Immer, E. Finkman, and J.-M. Gérard, *Appl. Phys. Lett.* **78**, 2327 (2001).

<sup>18</sup>A. Mohan, M. Felici, P. Gallo, B. Dwir, A. Rudra, J. Faist, and E. Kapon, *Nat. Photonics* **4**, 302 (2010).

<sup>19</sup>A. Mohan, P. Gallo, M. Felici, B. Dwir, A. Rudra, J. Faist, and E. Kapon, *Appl. Phys. Lett.* **98**, 253102 (2011).

<sup>20</sup>S. M. Kim and J. S. Harris, *Appl. Phys. Lett.* **85**, 4154 (2004).

<sup>21</sup>S. J. Lee, Z. Ku, A. Barve, J. Montoya, W.-Y. Jang, S. R. J. Brueck, M. Sundaram, A. Reisinger, S. Krishna, and S. K. Noh, *Nat. Commun.* **2**, 286 (2011).